THE JOURNAL OF BIOLOGICAL CHEMISTRY VOL. 283, NO. 21, pp. 14384–14390, May 23, 2008

Calcium Dynamics in the Peroxisomal Lumen of Living Cells*[S]

Received for publication, January 23, 2008, and in revised form, March 20, 2008 Published, JBC Papers in Press, March 24, 2008, DOI 10.1074/jbc.M800600200

Ilaria Drago[‡], Marta Giacomello[‡], Paola Pizzo[‡], and Tullio Pozzan[‡§1]

From the [‡]Department of Biomedical Sciences and Consiglio Nazionale delle Ricerche Institute of Neuroscience, University of Padua and [§]Venetian Institute of Molecular Medicine, 35121 Padua, Italy

We here describe the generation of novel, green fluorescent protein-based Ca^{2+} indicators targeted to the peroxisome lumen. We show that (i) the Ca^{2+} concentration of peroxisomes in living cells at rest is similar to that of the cytosol; (ii) increases in cytosolic Ca^{2+} concentration (elicited by either Ca^{2+} mobilization from stores or Ca^{2+} influx through plasma membrane Ca^{2+} channels) are followed by a slow rise in intraperoxisomal $[Ca^{2+}]$; (iii) Ca^{2+} influx into peroxisomes is driven neither by an ATP-dependent pump nor by membrane potential nor by a $H^+(Na^+)$ gradient. The peroxisomal membrane appears to play a low pass filter role, preventing the organelle from taking up shortlasting cytosolic Ca^{2+} transients but allowing equilibration of the peroxisomal luminal $[Ca^{2+}]$ with that of the cytosol during prolonged Ca^{2+} increases. Thus, peroxisomes appear to be an additional cytosolic Ca^{2+} buffer, but their influx and efflux mechanisms are unlike those of any other cellular organelle.

A variation in cytosolic Ca^{2+} is a key component of the cell signaling machinery activated by receptor stimulation. Although a plethora of information is available regarding Ca^{2+} dynamics in different subcellular compartments, a notable exception is represented by peroxisomes, single membrane-bound organelles diffusely distributed within the cytosol of virtually all eukaryotic cells (1). Proteins located in the peroxisomal matrix are linked to different biochemical pathways (2) such as the β-oxidation of fatty acids and detoxification of hydrogen peroxide. The latter pathway is exclusively localized in the peroxisomal compartment of fungi and plants, whereas in mammalian cells it is distributed between peroxisomes and mitochondria (2). Specialized peroxisomal functions, such as fatty acid degradation and synthesis of phytohormones, are found in some cells, (*e.g.* plants and fungi) (3). Interest in peroxisomes has increased recently due to the discovery that defects in peroxisomal biogenesis and peroxisomal enzyme deficiencies are linked to several genetic disorders in humans (4). Given that any enzymatic activity is highly sensitive to the ionic composition of the surrounding environment, it is surprising that information on the luminal ion content of peroxisomes is scarce and contradictory. In particular, no data are currently available on Ca^{2+} concentration in the peroxisome lumen, $[Ca^{2+}]_P$.

We here present a novel probe, derived from the new green fluorescent protein (GFP)[2]-based Ca^{2+} indicators (Dcpv) (5), for monitoring $[Ca^{2+}]_P$ in living cells. We show that peroxisomes contribute to the sequestration of part of the Ca^{2+} entering the cytoplasm during cell activation in a way that is unique among cellular organelles.

MATERIALS AND METHODS

Constructs—The sequence coding for the tripeptide SKL was introduced before the stop codon of D3cpv (kindly provided by R. Tsien, San Diego, CA) by PCR using the oligonucleotides 5′-ACCCAAGCTTGCCACCATG-3′ (forward); 5′-ACCCAAGCTTGCCACCATG-3′ (reverse). The resulting PCR product was digested with HindIII and EcoRI and ligated into pcDNA3 (Invitrogen). PCR for introducing the KVK coding sequence was performed using D3cpv-SKL as a template with the same forward primer and the following reverse: 5′-ACCCAAGCTTGCCACCATG-3′. The cDNA of pHluorin was a kind gift from S. Grinstein (Toronto, Canada).

Cell Culture and Transfection—HeLa cells were grown in Dulbecco's modified Eagle's medium containing 10% fetal calf serum supplemented with L-glutamine (2 mM), penicillin (100 units/ml), and streptomycin (100 μg/ml) in a humidified atmosphere containing 5% CO_2, while GH3 cells were grown in the same medium supplemented with non-essential amino acid (Sigma). Cells were seeded onto glass coverslips (24-mm diameter); for GH3 cells, coverslips were pretreated with poly-L-lysine (50 μg/ml). Transfections were performed at 60% confluence using TransIT®-LT1 transfection reagent (Mirus, Bologna, Italy) with 1 μg of DNA. Fluorescence experiments were performed 48 h after transfection.

Cell Loading with Fura-2, BCECF, or BAPTA—To monitor cytosolic $[Ca^{2+}]$ or pH, cells seeded on coverslips were incubated with 1 μM fura-2/AM or 2 μM BCECF/AM in an extracellular-like solution for 30 min at 37 °C, washed, and then incubated for 30 min at room temperature. In the experiments aimed at reducing cytosolic and organelle $[Ca^{2+}]$ to the lowest possible level, cells were loaded contemporaneously with 1 μM fura-2/AM and 10 μM BAPTA/AM using the protocol described above in a medium without $CaCl_2$ and supplemented with 500 μM EGTA.

* This work was supported in part by grants from Italian Telethon, AIRC (Italian Association for Cancer Research), the Cariparo Foundation (to T. P.), the University of Padua, and the Italian Ministry of University (FIRB 2004) (to P. P.). The costs of publication of this article were defrayed in part by the payment of page charges. This article must therefore be hereby marked "*advertisement*" in accordance with 18 U.S.C. Section 1734 solely to indicate this fact.

[S] The on-line version of this article (available at http://www.jbc.org) contains supplemental Fig. S1 and supplemental references and data.

[1] To whom correspondence should be addressed: Dept. of Biomedical Sciences, CNR Inst. of Neurosciences, University of Padua, Viale G Colombo 3, 35121 Padua, Italy. Tel.: 39-049-827-6067; Fax: 39-049-827-6049; E-mail: tullio.pozzan@unipd.it.

[2] The abbreviations used are: GFP, green fluorescent protein; TRH, thyrotropin-releasing hormone; BCECF, 2′,7′-bis-(2-carboxyethyl)-5-(and-6)-carboxyfluorescein; BAPTA, 1,2-bis(o-aminophenoxy)ethane-*N*,*N*,*N*′,*N*′-tetraacetic acid.

Cell Imaging—Cells expressing (or loaded with) the fluorescent probes were analyzed using an inverted fluorescence microscope (Zeiss Axioplan) with an immersion oil objective (×63, N.A. 1.40, for fluorescent probes and ×40, N.A. 1.3, for fura-2 and BCECF). Excitation light was produced by a monochromator (Polychrome II; TILL Photonics, Martinsried, Germany): 400 and 480 nm for pHluorin; 340 and 380 nm for fura-2; 495 and 440 nm for BCECF. The two excitation wavelengths were rapidly alternated and the emitted light deflected by dichroic mirrors (HQ 520 LP for pHluorin and BCECF and 455DRPL for fura-2) was collected through emission filters (HQ 520 LP for pHluorin and BCECF and 480 ELFP for fura-2). For the D3-derived probe, the excitation light was 425 nm. The emitted light was collected through a beamsplitter (OES s.r.l., Padua, Italy) (emission filters HQ 480/40M for cyan fluorescent protein and HQ 535/30 M for yellow fluorescent protein) and a dichroic mirror (515 DCXR). Filters and dichroic mirrors were purchased from Omega Optical and Chroma. Images were acquired using a cooled CCD camera (Imago; TILL Photonics) attached to a 12-bit frame grabber. Synchronization of the monochromator and CCD camera was performed through a control unit run by TILLvisION v.4.0 (TILL Photonics); this software was also used for image analysis. For time course experiments, the fluorescence intensity was determined over regions of interests covering small groups of peroxisomes or cytosolic regions (devoid of identifiable structures). Exposure time and frequency of image capture varied from 30 to 500 ms and from 5 to 0.2 Hz, respectively. Cells were mounted into an open-topped chamber thermostated at 37 °C and maintained in an extracellular medium containing (in mM): 135 NaCl, 5 KCl, 1 $MgSO_4$, 0.4 KH_2PO_4, 10 glucose, 20 Hepes, pH 7.4, at 37 °C. Plasma membrane permeabilization was performed by treating cells for 1 min with 100 μM digitonin in an intracellular-like medium containing (in mM): 130 potassium-gluconate, 10 NaCl, 1 KH_2PO_4, 1 $MgSO_4$, 20 Hepes, pH 7.0, at 37 °C and 500 μM EGTA. Experiments with permeabilized cells were performed in the same medium; where indicated, the latter was supplemented with a buffer containing (in mM): 2 EGTA, 1 H-EDTA, 1 $MgCl_2$, and variable $CaCl_2$ concentration.

Immunocytochemistry—Cells were fixed in phosphate-buffered saline containing 4% paraformaldehyde for 20 min, permeabilized with 0.1% Triton X-100 in phosphate-buffered saline containing 0.5% bovine serum albumin and 0.15% glycine (PBG) for 20 min, and blocked with 5% non-immune goat serum in PBG for 30 min. Rabbit anti-catalase (Rockland Immunochemicals, Gilbertsville, PA) or rabbit anti-PMP70 (Sigma) antibodies were added for 1 h at 37 °C. Samples were washed three times in PBG and then treated with Alexa Fluor 568 goat anti-rabbit IgG (Invitrogen) for 1 h at room temperature. Samples were washed three times in PBG and three times in phosphate-buffered saline, mounted with Mowiol (Sigma), and analyzed with a Leica TCS SP5 confocal microscope using an immersion oil objective (×63, N.A. 1.40). Image acquisition was performed by sequential scanning with excitation wavelengths of 488 nm for D3cpv-(KVK)-SKL and 543 nm for Alexa Fluor 568. Emission wavelengths were collected in the 495 to 535-nm (D3cpv-(KVK)-SKL) and 580 to 630-nm (Alexa Fluor 568) ranges. Correction of the bleed-through from the green fluorescence into the Alexa Fluor 568 channel and merging of the emitted fluorescence were carried out using the Acousto Optical Beam Splitter technique and the software provided by the manufacturer of the confocal microscope.

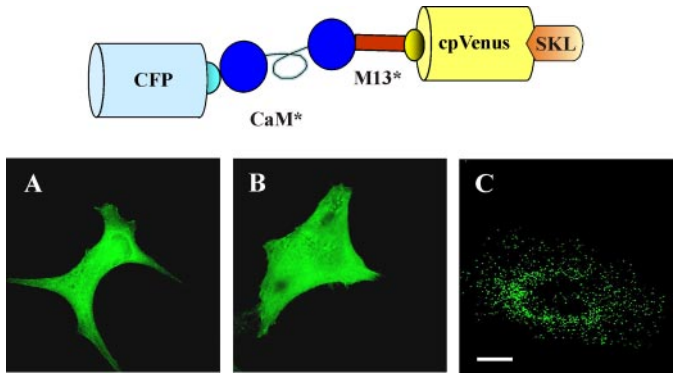

FIGURE 1. **Subcellular distribution of transiently expressed D3cpv-SKL in HeLa cells.** D3cpv, a new generation member of the Cameleon, fluorescence resonance energy transfer-based Ca^{2+} sensor family, carrying new mutations (*) in the Calmodulin (*CaM*) and M13 sequences (5), was modified by insertion at the C terminus of the peroxisome targeting signal SKL (*upper panel*). HeLa cells transiently expressing the new protein (*A*) or the original cytosolic probe (*B*) showed no difference in their subcellular distribution. Upon plasma membrane permeabilization with 100 μM digitonin (which results in complete release of the cytosolic probe), punctate structures scattered throughout the cytoplasm, later verified to be peroxisomes (see "Results" for details), became visible (*C*).

Materials—Cyclo piazonic acid, digitonin, carbonyl cyanide-4-(trifluoromethoxy)-phenylhydrazone, histamine, monensin, and thyrotropin-releasing hormone (TRH) were purchased from Sigma-Aldrich, ionomycin from Calbiochem, and fura-2/AM, BCECF/AM, and BAPTA/AM from Molecular Probes. All other materials were analytical or highest available grade.

Statistical Analysis—All the data are representative of at least five different experiments. Values are expressed as mean ± S.E.

RESULTS

Peroxisome Targeting of the GFP-based Ca^{2+} Indicator—Fig. 1, *top*, shows the schematic structure of D3cpv, modified by the insertion at the C-terminal of the canonical peroxisomal targeting signal, the tripeptide Ser-Lys-Leu (*SKL*) (6). Although this sequence is known to be efficacious in targeting several recombinant proteins to peroxisomes, the D3cpv-SKL subcellular distribution (Fig. 1*A*) in HeLa cells transiently expressing the construct was indistinguishable from that of cytosolic D3cpv (Fig. 1*B*). Treatment of cells with digitonin, although releasing all cytosolic D3cpv (not shown), revealed that a fraction of the D3cpv-SKL was trapped in numerous small structures scattered throughout the cytoplasm (Fig. 1*C*). The D3cpv-SKL-positive spots coincide with peroxisomes, as revealed by their positivity after immunostaining with antibodies for markers of these organelles, catalase (Fig. 2*B*) or the peroxisomal membrane protein 70 (Fig. 2*E*). The missorting of D3cpv-SKL was observed in all other cell types investigated, GH3, Chinese hamster ovary, and SH-SY5Y. The cytoplasmic staining was not due to protein overexpression and saturation of the peroxisome protein import mechanism, because the same results were obtained when transfection was carried out with only 1/5 of the cDNA or if the cells were observed 48, 72, or 96 h after transfection (not shown).

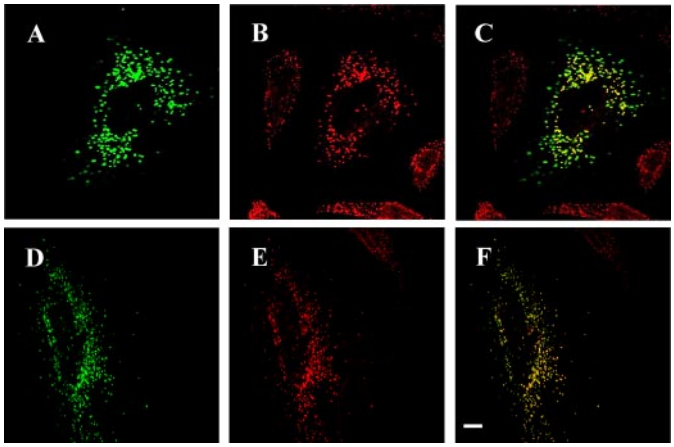

FIGURE 2. **D3cpv-SKL co-localizes after cell membrane permeabilization with the peroxisome protein markers, catalase and PMP70.** HeLa cells transiently expressing D3cpv-SKL were permeabilized with digitonin (*A* and *D*). Cells were then fixed and treated with an antibody against a peroxisome marker, catalase (*B*) or PMP70 (*E*) and then with a secondary antibody conjugated to Alexa 568. Co-localization of the two signals is shown in *C* and *F*. *Scale bar*, 10 μm.

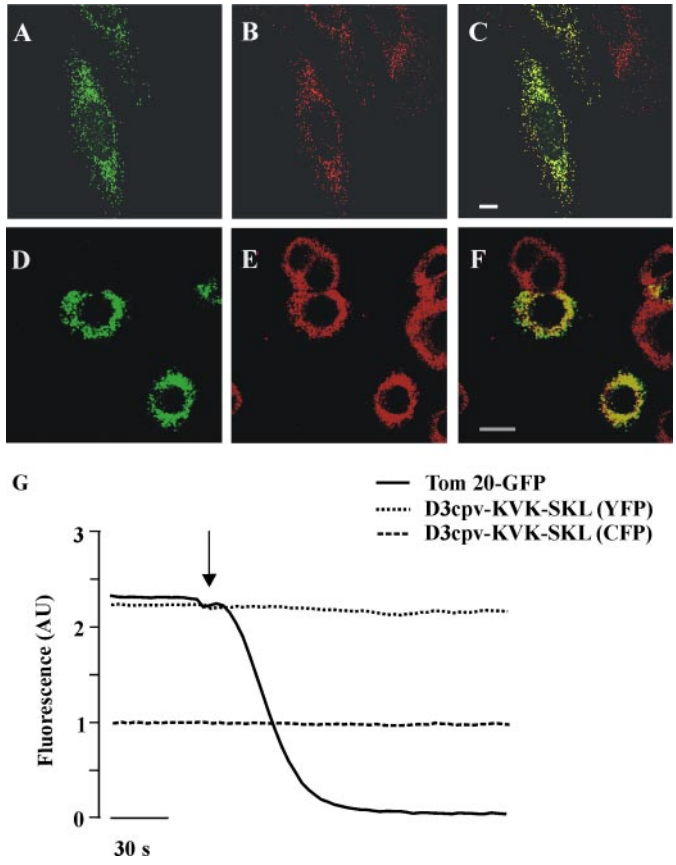

FIGURE 3. **Subcellular localization of transiently expressed D3cpv-KVK-SKL in HeLa and GH3 cells.** Confocal images of HeLa (*A*) or GH3 cells (*D*) transiently expressing D3cpv-KVK-SKL. In *B* and *E*, the immunolocalization of the peroxisome membrane protein PMP70 is presented. In *C* and *F*, the colocalization of the two signals is coded as *yellow*. For details, see "Materials and Methods." *Scale bar*, 10 μm. *G*, HeLa cells transiently expressing either D3cpv-KVK-SKL or TOM20-GFP, a fluorescent protein linked to the outer mitochondrial membrane and facing the cytosol, were permeabilized with digitonin in an intracellular-like medium and treated with proteinase K (see "Materials and Methods"). GFP fluorescence (*continuous trace*), yellow fluorescent protein fluorescence (*YFP*) (*dotted trace*), and cyan fluorescent protein fluorescence (*CFP*) (*dashed trace*) are presented (*AU*, arbitrary units). The *arrow* indicates Proteinase K addition. Similar experiments were carried out in GH3 cells with identical results.

To improve the peroxisome localization, a novel construct was made where the C-terminal SKL was preceded by a three-amino acid positively charged sequence, Lys-Val-Lys (KVK). This sequence was designed to fit the requirement for improved peroxisomal targeting described by Neuberger *et al.* (7, 8) (Fig. 3*A*). The majority of cells transfected with D3cpv-KVK-SKL were characterized by the presence only of punctate fluorescence, with a negligible signal in the cytosol. A small percentage of cells (5–30%) still revealed cytosol missorted probe. Such increase in targeting efficiency was observed also in Chinese hamster ovary, SH-SY5Y (not shown), and GH3 cells (Fig. 3*D*). Immunostaining with anti-PMP70 antibody revealed that all the D3cpv-KVK-SKL-positive vesicles of HeLa and GH3 cells are also positive for the *bona fide* peroxisome marker (Fig. 3, *C* and *F*).

The experiment presented in Fig. 3*G* was aimed at determining whether the Ca^{2+} probe was trapped within the peroxisome lumen or whether it was bound to the cytosolic surface of peroxisomes. The plasma membrane of HeLa cells was permeabilized with digitonin, and the cells were then treated with Proteinase K. The protease did not affect the D3cpv-KVK-SKL fluorescent signal, whereas, on the contrary, in cells expressing a GFP construct localized on the cytosolic surface of the outer mitochondrial membrane, TOM20-GFP (9), the enzyme abolished the fluorescence in a few seconds. Similar results were obtained in GH3 cells (not shown).

Ca^{2+} Handling by Peroxisomes in Intact Cells—We used as a first model system GH3 cells because these cells are endowed with (i) abundant plasma membrane voltage-gated Ca^{2+} channels and (ii) endogenous receptors (TRH receptors) coupled to inositol 1,4,5-trisphosphate production and Ca^{2+} mobilization from stores (10). Fig. 4*A* shows the typical response pattern of the D3cpv-KVK-SKL fluorescence signal of three GH3 cells to depolarization with 30 mM KCl. In two cells, the fluorescence was exclusively in peroxisomes, whereas in the third cell fluorescence was diffuse throughout the whole cytosol. Cell depolarization caused an increase in the fluorescence emitted at 540 nm and a decrease of the signal at 480 nm (not shown) and thus an increase in the 540/480-nm fluorescence emission ratio (here presented as $\Delta R/R_0$), which is proportional to $[Ca^{2+}]$ (Fig. 4*A*). The kinetics of the $\Delta R/R_0$ changes were, however, different in the cells where the probe was localized in the peroxisomes and in the cell with the mistargeted indicator. The cytosolic $\Delta R/R_0$ (*continuous line*) reached the peak in 1–2 s and then started to decrease slowly; the peroxisome signal, on the contrary, reached the peak in 10–15 s and then started to decline. Addition of EGTA accelerated the drop to basal level of both the cytosolic and peroxisomal signals, the effect on the cytosol being more evident. In Fig. 4*B*, the fluorescence emission ratio (excitation 340/380 nm) of a parallel batch of cells loaded with the Ca^{2+} indicator fura-2 is presented. The kinetics of the fura-2 signal were similar to that of cells expressing the missorted D3cpv-KVK-SKL probe (Fig. 4*A*). Similar data were obtained with cells expressing the original cytosolic D3cpv (not shown). In the experiment presented in Fig. 4*C* the peak levels reached by $[Ca^{2+}]_p$, expressed as percentage of the maximal

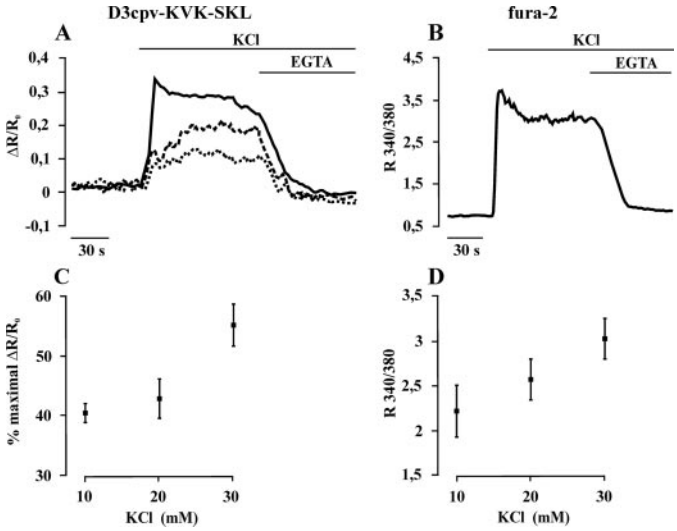

FIGURE 4. **Peroxisome Ca^{2+} increases in GH3 cells.** Kinetics of the fluorescence changes of typical GH3 cells transiently expressing (i) D3cpv-KVK-SKL, selectively within peroxisomes (*A*, two cells, *dashed* and *dotted traces*), (ii) mistargeted to the cytosol (*A*, *continuous trace*), or (iii) loaded with fura-2 (*B*). Where indicated, 30 mM KCl and 2 mM EGTA were added in a Ca^{2+}-containing medium. When 30 mM NaCl was added instead of KCl, no effect on either cytosolic or peroxisomal $[Ca^{2+}]$ was recorded. Data are plotted as $\Delta R/R_0$, where R_0 is the fluorescence emission ratio (*R* 540/480 nm) at time 0 and ΔR is the increase in fluorescence emission ratio at any point. For fura-2 measurements, the ratio of the light intensity emitted at 505 nm upon dye excitation at the two wavelengths (*R* 340/380) is a function of the cytosolic $[Ca^{2+}]$ and is displayed on the *left side* of the panel in this and the following figures. *D*, mean rises in the *R* 340/380-nm fluorescence excitation ratio of the fura-2 signal as a function of KCl concentration. The mean rises in peroxisome Ca^{2+} level (*C*), expressed as percentage of the 540/480 maximal $\Delta R/R_0$, show a similar trend. Mean of 15 (*C*) or 19 (*D*) experiments ± S.E. For details, see "Materials and Methods."

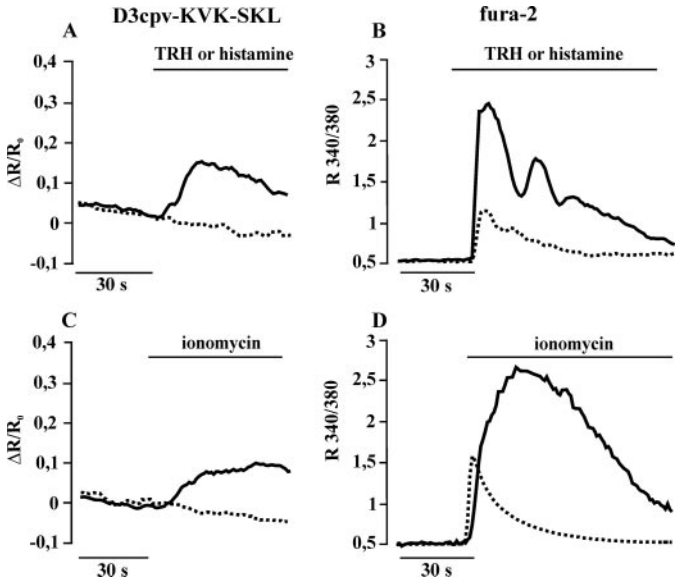

FIGURE 5. **Ca^{2+} release from stores causes a peroxisomal Ca^{2+} rise in HeLa, but not in GH3, cells.** Kinetics of the fluorescence changes of a typical HeLa cell (*continuous trace*) or GH3 cell (*dotted trace*) transiently expressing D3cpv-KVK-SKL in peroxisomes (*A* and *C*) or loaded with fura-2 (*B* and *D*). Where indicated, ionomycin (100 nM), the inositol 1,4,5-trisphosphate-generating agonist histamine (100 μM), for HeLa cells, or TRH (1 μM) for GH3 cells was added in a Ca^{2+}-free medium. For details, see "Materials and Methods."

$\Delta R/R_0$, are plotted as a function of KCl concentration. For comparison, in Fig. 4*D* the 340/380 nm emission ratio of cells loaded with fura-2 is also shown. It is clear that the peak rise in peroxisomal and fura-2 signals showed a similar dependence on [KCl]. Confirming that the $[Ca^{2+}]_p$ increase depends on the cytosolic $[Ca^{2+}]$ rise, when KCl was added in a medium devoid of Ca^{2+} no increase in peroxisome and cytosolic $[Ca^{2+}]$ was observed (not shown).

The question then arises as to the behavior of peroxisomes, in terms of Ca^{2+} response, to agents that cause Ca^{2+} mobilization from intracellular stores, either elicited by TRH or by the Ca^{2+} ionophore ionomycin, both added in the absence of extracellular Ca^{2+}. The two agents caused neither a drop nor a rise in $[Ca^{2+}]_p$ (under conditions that elicited significant transient Ca^{2+} rises, as measured with fura-2; compare Fig. 5, *A* and *C*, with Fig. 5, *B* and *D*, *dotted traces*). When TRH or ionomycin was added after a previous pulse of KCl (to overload Ca^{2+} stores), the percentage of peroxisomal Ca^{2+} increases in response to TRH and ionomycin increased significantly (20 and 53% of cells, respectively; not shown). The problem of the peroxisomal behavior in response to Ca^{2+}-mobilizing stimuli was then further addressed in HeLa cells treated with histamine or ionomycin (Fig. 5). In all cells investigated, histamine induced a cytosolic $[Ca^{2+}]$ rise, as measured with fura-2 (Fig. 5*B*, *continuous trace*), whereas in 68% of cells the peroxisome signal also increased significantly (Fig. 5*A*, *continuous trace*). In HeLa cells, addition of ionomycin in Ca^{2+}-free medium (which resulted in a large cytosolic $[Ca^{2+}]$ increase in all cells tested; Fig. 5*D*, *continuous trace*) always resulted in a rise of $[Ca^{2+}]_p$ (Fig. 5*C*, *continuous trace*).

Mechanism of Ca^{2+} Transport in Peroxisomes—The Ca^{2+} rise within peroxisomes induced by KCl-dependent depolarization in GH3 cells was indistinguishable in the presence or absence of mitochondrial uncouplers or of sarcoendoplasmic reticulum Ca^{2+} ATPase inhibitors (not shown). Given that no reliable inhibitor of the Golgi-type pump is available, to verify the involvement of ATP-dependent uptake mechanisms we investigated the effects of ATP on the rate and extent of $[Ca^{2+}]_p$ rise in digitonin-permeabilized cells exposed to a medium with 500 nM Ca^{2+}. As shown in Fig. 6*A*, Ca^{2+} uptake was similar with (*continuous trace*) and without (*dotted trace*) an energy source. Notably, when an excess EGTA was added (to rapidly decrease medium $[Ca^{2+}]$), the peroxisome $[Ca^{2+}]$ decreased with relatively slow kinetics (Fig. 6*B*) To test whether peroxisomal Ca^{2+} influx depends on the presence of a classical Ca^{2+} channel, digitonin-permeabilized cells were treated with 10 μM La^{3+}, a nonspecific inhibitor of several Ca^{2+} channels. The increase in $[Ca^{2+}]_p$ upon increase in medium $[Ca^{2+}]$ to 500 nM or 5 μM was unaffected by La^{3+} (not shown).

We then investigated whether peroxisomal Ca^{2+} uptake may depend on a $Na^+(H^+)/Ca^{2+}$ antiport. Intact GH3 cells were pretreated with either NH_4Cl (Fig. 6*C*, *dotted trace*), an agent that causes an alkalinization of organelle pH, or monensin (*dashed trace*), a H^+/Na^+ exchange ionophore, which should collapse any gradient of either Na^+ or H^+ across the peroxisomal membrane, if they exist. Neither NH_4Cl nor monensin had any appreciable effect on the $[Ca^{2+}]_p$ increase caused by 30 mM KCl. Similar results were obtained in HeLa cells stimulated with either histamine or ionomycin (not shown).

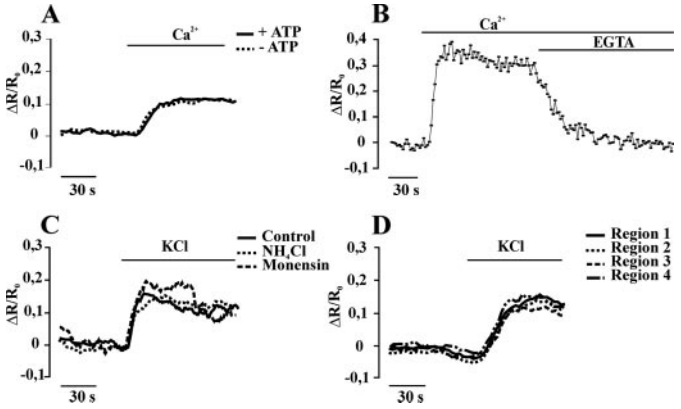

FIGURE 6. **Effects of ATP, H^+, or Na^+ gradients on peroxisomal Ca^{2+} uptake in GH3 cells and homogeneous responses of peroxisomes within a cell to a cytosolic Ca^{2+} rise.** *A*, GH3 cells transiently expressing D3cpv-KVK-SKL were permeabilized with digitonin in an intracellular-like medium, described under "Materials and Methods," with (*continuous trace*) or without (*dotted trace*) 200 μM ATP and 2 mM succinate. After digitonin washout, the cells were superfused with medium whose [Ca^{2+}] was buffered at 500 nM. *B*, the same conditions as *A* where indicated 150 μM Ca^{2+} and 250 μM EGTA were added. *C*, intact GH3 cells expressing D3cpv-KVK-SKL selectively in peroxisomes were treated with 10 mM NH_4Cl (*dotted trace*) or 5 μM monensin (*dashed trace*) 30 s before inducing depolarization with 30 mM KCl. *D*, kinetic changes of $\Delta R/R_0$ of four different groups of peroxisomes within the same GH3 cell are presented. Cell was stimulated with 30 mM KCl in a Ca^{2+}-containing medium.

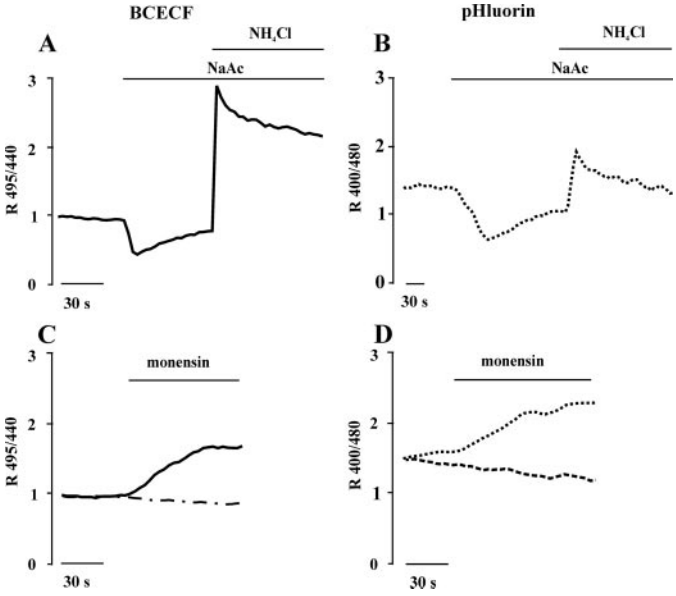

FIGURE 7. **Measurement of peroxisome luminal pH.** GH3 cells loaded with the cytosolic pH indicator BCECF (*A* and *C*) or transiently expressing the peroxisomal pH probe pHluorin (*B* and *D*) were challenged where indicated with $NaCH_3CO_2$ (NaAc, 30 mM), NH_4Cl (30 mM), or monensin (5 μM) in a Ca^{2+}-containing medium. For *C* and *D* (*dashed-dot* and *dashed traces*), the pH of the extracellular medium was decreased to 7.0, NaCl was iso-osmotically substituted with KCl, $CaCl_2$ was omitted, and 100 μM EGTA was added instead. For further details, see "Materials and Methods."

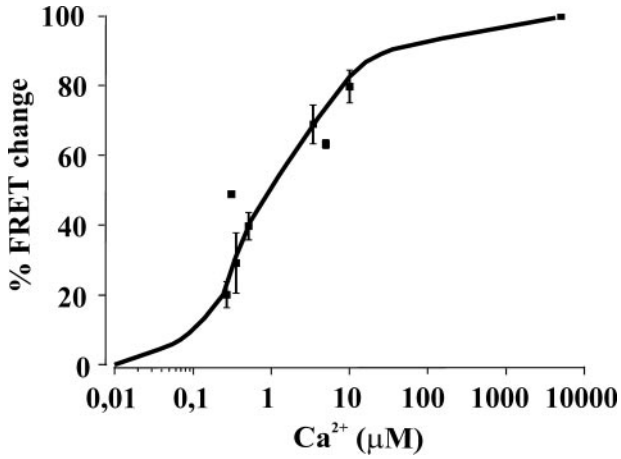

FIGURE 8. ***In situ* calibration of D3cpv-KVK-SKL fluorescence as a function of [Ca^{2+}].** GH3 cells transiently expressing D3cpv-KVK-SKL were permeabilized with digitonin in an intracellular-like medium supplemented with 100 μM EGTA and devoid of ATP and succinate. The value of 540/480 nm fluorescence emission ratio under these conditions was assumed to represent R_{min}. The cells were then superfused with medium whose [Ca^{2+}] was buffered (with EGTA) at different levels up to a concentration of 3 μM Ca^{2+}. The values of [Ca^{2+}] above 3 μM were obtained by simply adding $CaCl_2$ at the indicated concentrations to medium without EGTA. R_{max} was determined by addition of 5 mM $CaCl_2$. As described in the supplemental material, the values of *R* at the different Ca^{2+} concentration of independent experiments were normalized based on the observation that the R_{max}/R_{min} ratio is constant in different cells. The normalized *R* values (mean ± S.E.) were then plotted as a function of the [Ca^{2+}] ($n = 37$).

To verify whether there are heterogeneities among the organelles, the [Ca^{2+}] rise in different groups of peroxisomes was next investigated. As shown in Fig. 6*D*, the response to a 30-mM KCl challenge of different groups of organelles within the same GH3 cell was found to be very similar. Identical results were obtained in HeLa cells using either ionomycin or histamine as the stimulus (not shown).

Finally, the peroxisome lumenal pH was directly monitored using the targeted pH indicator pHluorin (see "Materials and Methods" and Ref. 11). Cytosolic pH was measured in parallel with BCECF (12). Fig. 7 shows that the weak acid acetate caused a reduction of both cytoplasmic (Fig. 7*A*) and peroxisomal (Fig. 7*B*) pH, whereas NH_4Cl caused an alkalinization of both compartments. Monensin also caused an increase of pH both in the cytosol (Fig. 7*C*, *continuos trace*) and in peroxisomes (Fig. 7*D*, *dotted trace*). When the cells were incubated in a medium where NaCl was iso-osmotically substituted with KCl (to abolish the Na^+ gradient across the plasma membrane and in the absence of Ca^{2+} to block Ca^{2+} influx) and the extracellular pH was dropped to 7.0 (to reduce the pH gradient), monensin hardly modified cytosolic pH (Fig. 7*C*, *dashed point trace*) and in parallel failed to cause any significant change in peroxisomal pH (Fig. 7*D*, *dashed trace*).

Calibration of the Peroxisomal [Ca^{2+}]—To determine the absolute values of $[Ca^{2+}]_p$, the *in situ* K_d for Ca^{2+} of D3cpv-KVK-SKL was determined using the passive Ca^{2+} loading procedure previously described (13). Transfected cells were permeabilized with digitonin in an intracellular-like medium, but devoid of ATP or any mitochondrial oxidizable substrate, and variable concentration of Ca^{2+} (see "Materials and Methods"). The percentage of the normalized 540/480-nm fluorescence emission ratio changes at steady state were then plotted as a function of medium [Ca^{2+}] (Fig. 8). The apparent K_d for Ca^{2+}, as calculated *in situ*, 1.0 μM, is not much different from that calculated *in vitro* with recombinant D3cpv, 0.6 μM (5). A detailed description of the protocol employed to calculate the [Ca^{2+}] within peroxisomes is presented in supplemental data. A summary of the absolute values of $[Ca^{2+}]_p$ (as measured with D3cpv-KVK-SKL), compared with the cytosolic Ca^{2+} values (as

TABLE 1
$[Ca^{2+}]$ in cytosol and peroxisome lumen upon addition of different stimuli

Conditions as in Figs. 5 and 6. Mean of 61 (*fura-2*) and 38 (*D3cpv-KVK-SKL*) experiments ± S.E.

Stimulus	Cell type	Ca^{2+} fura-2	S.E.	Ca^{2+} D3cpv-KVK-SKL	S.E.
		μM	μM	μM	μM
KCl (10 mM)	GH3	1.79	0.47	0.52	0.08
KCl (20 mM)	GH3	2.01	0.41	0.64	0.10
KCl (30 mM)	GH3	3.34	0.84	1.32	0.25
histamine (100 μM)	HeLa	1.31	0.13	0.72	0.11
Ionomycin (100 nM)	HeLa	1.33	0.59	0.76	0.11

measured in parallel by fura-2), is presented in Table 1. The $[Ca^{2+}]_p$ at rest, both in HeLa and GH3 cells, is ~150 nM, *i.e.* not significantly different from that measured with fura-2 (150 and 190 nM for GH3 and HeLa cells, respectively). The mean $[Ca^{2+}]_p$ peak of GH3 cells (upon stimulation with 30 mM KCl), 1.32 ± 0.25 μM, compares to 3.34 ± 0.84 μM measured with fura-2. The averaged $[Ca^{2+}]_p$ peaks in HeLa cells stimulated with histamine or ionomycin (both added in Ca^{2+}-free medium) are 0.72 ± 0.11 and 0.76 ± 0.11 μM compared with cytosolic peaks of 1.31 ± 0.13 and 1.33 ± 0.59 μM, respectively.

DISCUSSION

The most common peroxisome-targeting mechanism involves the C terminus tripeptide SKL (6). When this sequence was added to the GFP-based Ca^{2+} indicators D1- and D3cpv (5) most of the transfected protein mislocalized to the cytosol. Inclusion of a longer targeting sequence (KVK-SKL), however, resulted in more satisfactory peroxisome localization. The expressed protein is clearly trapped in the lumen of the organelles, as demonstrated by its resistance to proteolytic cleavage and by the slower kinetics of the fluorescence signal changes in response to a sudden change in extraperoxisomal $[Ca^{2+}]$.

When cytosolic $[Ca^{2+}]$ was increased in GH3 cells by depolarizing the plasma membrane with high KCl, the $[Ca^{2+}]_p$ also raised, although with slower kinetics. The amplitude of the $[Ca^{2+}]_p$ increase paralleled that of the cytosol. In quantitative terms, the maximum rises of $[Ca^{2+}]_p$ after depolarization were lower than those calculated with the classical cytosolic indicator fura-2. Considering the inherent assumptions involved in the calibration procedures of the two probes, it can be safely concluded that $[Ca^{2+}]_p$ tends to equilibrate with the cytosolic $[Ca^{2+}]$ and no driving force (ATP and/or $Na^+(H^+)$ gradients) leads to Ca^{2+} influx into peroxisomes. In support of this conclusion, the luminal pH of peroxisomes is practically indistinguishable from that of the cytoplasm, and monensin never caused an acidification of peroxisomal lumen, demonstrating that $[Na^+]$ of peroxisomes is similar to that of cytoplasm. Our conclusion concerning the lack of any significant gradient of H^+ across the peroxisomal membrane concurs with Jankowski *et al.* (11), whereas other groups have reported that the intraperoxisome pH is slightly alkaline in mammalian cells (14) or in yeasts slightly acidic (15) or alkaline (16, 17).

A permeability barrier to Ca^{2+} diffusion across the peroxisome membrane, however, does exist as demonstrated by these results: (i) the rate of peroxisome Ca^{2+} rise in intact cells treated with KCl is substantially slower than in the cytosol, and (ii) in permeabilized cells, sudden changes in medium $[Ca^{2+}]$ require several seconds to equilibrate with the organelle lumen. Surprisingly, whereas increases in cytosolic $[Ca^{2+}]$ elicited in GH3 cells by Ca^{2+} influx though voltage-gated Ca^{2+} channels were followed by $[Ca^{2+}]_p$ rises, Ca^{2+} mobilization from internal stores, as induced by stimulation of TRH receptors, almost never resulted in a significant increase in $[Ca^{2+}]_p$. Even unspecific Ca^{2+} mobilization from stores, as promoted by ionomycin added in Ca^{2+}-free medium, was unable to induce Ca^{2+} uptake into peroxisomes of GH3 cells. The possibility was thus considered that the poor response of the peroxisomes to Ca^{2+} mobilization in GH3 cells reflects (i) the existence of a mechanism that prevents Ca^{2+} uptake in peroxisomes in response to Ca^{2+} mobilization from stores or (ii) a combination of the small and transient nature of the cytosolic Ca^{2+} rise in response to TRH (and ionomycin) in GH3 cells and of the slow Ca^{2+} uptake rate by peroxisomes. In other words, the small and transient rise in cytosolic $[Ca^{2+}]$ (as that elicited in GH3 cells by TRH or ionomycin) can be hardly coped with by the relatively slow Ca^{2+} uptake system of peroxisomes. The cytoplasmic $[Ca^{2+}]$ rise in response to depolarization, instead, does reach the peak in 2–3 s, but it is followed by a prolonged plateau level that lasts several tens of seconds. In support of the latter explanation, the very rapid Ca^{2+} increases due to spontaneous action potential firing (and Ca^{2+} influx through voltage-gated Ca^{2+} channels) often observed in GH3 cells (18) were never followed by significant increases in $[Ca^{2+}]_p$.

To distinguish between these possibilities, we used a different cell type, HeLa, where Ca^{2+} mobilization from stores in response to an inositol 1,4,5-trisphosphate-generating agonist, such as histamine, results in larger and relatively more prolonged Ca^{2+} transients compared with GH3 cells (peak values measured with fura-2 of 1.31 μM and 270 nM, back to basal levels in 120 and 50 s, in HeLa and GH3 cells, respectively). Indeed, we found that in HeLa cells the percentage of peroxisome responses to histamine application was much higher than that observed in GH3 cells in response to TRH (68 *versus* 1%, respectively) and the percentage of $[Ca^{2+}]_p$ increases in response to ionomycin was close to 100% in HeLa cells compared with <5% in GH3 cells. Thus, it may be concluded that, due to the intrinsic sluggish response to a cytosolic Ca^{2+} rise, peroxisomes are relatively insensitive to rapid transients of cytosolic $[Ca^{2+}]$ but significantly increase their Ca^{2+} level only in response to prolonged cellular Ca^{2+} increases. We cannot exclude, however, that peroxisomes of HeLa cells are more efficient than those of GH3 cells at taking up Ca^{2+}. However, when in GH3 cells TRH- or ionomycin-induced cytosolic Ca^{2+} increases are larger and more prolonged (as occurs when they are applied after KCl), the percentage of peroxisomal responses increases drastically (from 1 to 21% for TRH and from 5 to 53% with ionomycin), suggesting that the first explanation is most likely.

The final question concerns the heterogeneity of peroxisomal Ca^{2+} responses. When groups of organelles in the same cell were compared, no significant difference, either in kinetics or in amplitude of the Ca^{2+} responses, was ever observed. It cannot

be excluded, however, that single organelles localized in the proximity of Ca^{2+} channels of either the plasma membrane or the endoplasmic reticulum may experience larger local Ca^{2+} rises and, accordingly, undergo larger Ca^{2+} increases.

In conclusion, we have developed novel GFP-based Ca^{2+} indicators that can efficiently target to the peroxisomal lumen. These allow, for the first time to our knowledge, the measurement of this parameter in intact living cells. Taken together, the present data demonstrate that peroxisomes participate in the Ca^{2+} signaling pathway but their behavior is unlike that of any other organelle. In particular, peroxisomes do not act as Ca^{2+} stores from which Ca^{2+} can be mobilized upon stimulation, as the endoplasmic reticulum, the Golgi apparatus or, in some cells, acidic compartments (19). The Ca^{2+} response of peroxisomes to a rise in cytosolic $[Ca^{2+}]$ is also markedly different from that of mitochondria, in as much as their luminal Ca^{2+} does not increase as massively as that of the latter organelles. The organelle that most resembles peroxisomes in terms of Ca^{2+} response is the nucleus, although in the latter the kinetics of Ca^{2+} equilibration with the cytosol are 10–100-fold faster. Thus, because of this relatively slow Ca^{2+} influx, very rapid and transient increases in cytosolic Ca^{2+} may not lead to appreciable changes in $[Ca^{2+}]_p$, whereas more sustained increases will always lead to an increase in $[Ca^{2+}]_p$. It remains to be established whether and which reactions within the peroxisomes are affected by Ca^{2+}.

The amount of Ca^{2+} that is sequestered by peroxisomes will depend on (i) their number and volume (which may vary among different cells and in response to specific stimuli, *e.g.* peroxisome proliferator-activated receptor γ gene activation) and (ii) the endogenous Ca^{2+} buffering capacity of the organelles, which is presently unknown. In addition to a potential role as a cytosolic Ca^{2+} buffer, the increases in $[Ca^{2+}]_p$ may be relevant for the organelle's own functions. Thus far, potential candidates are the peroxisomal Ca^{2+}-dependent members of the mitochondrial carrier superfamily that contains four EF-hand Ca^{2+} binding domains (20) or a Ca^{2+}/calmodulin-regulated catalase isoform found in plant peroxisomes (21). The search for Ca^{2+}-modulated peroxisomal proteins may now be launched on a firmer ground, given the direct demonstration of the participation of these organelles in cellular Ca^{2+} handling.

Acknowledgment—We thank Paulo Magalhães for critically reading the manuscript and Paul Lazarow for helpful discussion.

REFERENCES

1. Platta, H. W., and Erdmann, R. (2007) *Trends Cell Biol.* **17,** 474–484
2. Poirier, Y., Antonenkov, V. D., Glumoff, T., and Hiltunen, J. K. (2006) *Biochim. Biophys. Acta* **1763,** 1413–1426
3. Goepfert, S., and Poirier, Y. (2007) *Curr. Opin. Plant Biol.* **10,** 245–251
4. Shimozawa, N. (2007) *J. Inherit. Metab. Dis.* **30,** 193–197
5. Palmer, A. E., Giacomello, M., Kortemme, T., Hires, S. A., Lev-Ram, V., Baker, D., and Tsien, R. Y. (2006) *Chem. Biol.* **13,** 521–530
6. Gould, S. J., Keller, G. A., Hosken, N., Wilkinson, J., and Subramani, S. (1989) *J. Cell Biol.* **108,** 1657–1664
7. Neuberger, G., Maurer-Stroh, S., Eisenhaber, B., Hartig, A., and Eisenhaber, F. (2003) *J. Mol. Biol.* **328,** 567–579
8. Neuberger, G., Maurer-Stroh, S., Eisenhaber, B., Hartig, A., and Eisenhaber, F. (2003) *J. Mol. Biol.* **328,** 581–592
9. Kanaji, S., Iwahashi, J., Kida, Y., Sakaguchi, M., and Mihara, K. (2000) *J. Cell Biol.* **151,** 277–288
10. Pizzo, P., Fasolato, C., and Pozzan, T. (1997) *J. Cell Biol.* **138,** 355–366
11. Jankowski, A., Kim, J. H., Collins, R. F., Daneman, R., Walton, P., and Grinstein, S. (2001) *J. Biol. Chem.* **276,** 48748–48753
12. Tsien, R. Y., Pozzan, T., and Rink, T. J. (1982) *J. Cell Biol.* **94,** 325–334
13. Rudolf, R., Magalhaes, P. J., and Pozzan, T. (2006) *J. Cell Biol.* **173,** 187–193
14. Dansen, T. B., Wirtz, K. W., Wanders, R. J., and Pap, E. H. (2000) *Nat. Cell Biol.* **2,** 51–53
15. Lasorsa, F. M., Scarcia, P., Erdmann, R., Palmieri, F., Rottensteiner, H., and Palmieri, L. (2004) *Biochem. J.* **381,** 581–585
16. Waterham, H. R., Keizer-Gunnink, I., Goodman, J. M., Harder, W., and Veenhuis, M. (1990) *FEBS Lett.* **262,** 17–19
17. van Roermund, C. W., de Jong, M., IJlst, L., van Marle, J., Dansen, T. B., Wanders, R. J., and Waterham, H. R. (2004) *J. Cell Sci.* **117,** 4231–4237
18. Schlegel, W., Winiger, B. P., Mollard, P., Vacher, P., Wuarin, F., Zahnd, G. R., Wollheim, C. B., and Dufy, B. (1987) *Nature* **329,** 719–721
19. Rizzuto, R., and Pozzan, T. (2006) *Physiol. Rev.* **86,** 369–408
20. Weber, F. E., Minestrini, G., Dyer, J. H., Werder, M., Boffelli, D., Compassi, S., Wehrli, E., Thomas, R. M., Schulthess, G., and Hauser, H. (1997) *Proc. Natl. Acad. Sci. U. S. A.* **94,** 8509–8514
21. Yang, T., and Poovaiah, B. W. (2002) *Proc. Natl. Acad. Sci. U. S. A.* **99,** 4097–4102